Research Journal of Applied Sciences, Engineering and Technology 10(6): 707-715, 2015
DOI:10.19026/rjaset.10.2481
ISSN: 2040-7459; e-ISSN: 2040-7467

Submitted: January 21, 2015 Accepted: March 4, 2015 Published: June 20, 2015

Research Article

Comparison of Modulation Techniques for Underwater Optical Wireless Communication Employing APD Receivers

Mazin Ali A. Ali
Department of Physics, College of Science, Al-Mustansiriyah University, Baghdad, Iraq

Abstract: In this study, we theoretically analyze the performance of an underwater optical wireless communications system using different modulation techniques and an avalanche photodiode APD receiver over underwater environment channels. Based on the LOS geometrical model and combined with signal to noise ratio model for Si and Ge APD and BER; then the impact of the distance of transmission and power of the transmitter and Jerlov water type are analyzed. The characteristics of bit error rate BER for different optical modulation techniques are studied. Simulation results indicate that the performance of H-QAM is more suited for an underwater optical wireless communication. On the other hand, the suitability of avalanche photodiodes under these modulation techniques is discussed, because the photodiode Si APD has more advantages compared with Ge APD when used in an underwater optical communication.

Keywords: Avalanche photodiode APD, bit error rate BER, modulation, underwater optical communication

INTRODUCTION

It is well known that radio frequencies cannot be used in water because they are strongly attenuated, allowing typical ranges of a few centimeters only. Use of acoustic waves is also problematic due to their limited bandwidth and very low celerity, as well as the high amount of energy consumed by large antennas used (Shah, 2009; Pignieri *et al*., 2008). Optical underwater communication is a cost-effective and low energy consumption solution that can provide high data rates over relatively short transmission ranges and has received a great deal of attention for the last few years (Gabriel *et al*., 2011). Optical transmittance in an underwater medium such as clear, ocean, turbid and harbor or other types will show big variation when examined versus the wavelength. The large information bandwidth available at visible wavelengths has also opened the possibility for high-speed, wireless communications in the underwater environment. Unfortunately, the propagation of light underwater is affected by both absorption and scattering (Mullen *et al*., 2009). While blue-green wavelengths can be used to minimize absorption in water, the scattering process tends to broaden the once collimated laser beam but there is no change in energy (Mobley, 1994). Absorption coefficient α (λ) and scattering coefficient β (λ) in units of inverse meter are used to determine the energy loss of non-scattered light caused by absorption and scattering, respectively. The attenuation coefficient indicates the total effects of absorption and scattering on energy loss as shown in Fig. 1 (Gawdi, 2006). The values of c (λ) depend on both the wavelength λ as well as turbidity of water (Tang *et al*., 2013).

The study is organized as follows. First, cover a briefly present underwater optical properties, a light propagation in water, Jerlov water types and line of sight transmission of light in water. Next, we present some results to study the performance of underwater optical communication such as: receiver signal power, SNR and BER. Finally, concluded in the last study.

Light propagation in water: When a photon is transmitted through water there are two mechanisms that prevent it from reaching a receiver further along the channel. The first is absorption $\alpha(\lambda)$ and the second is scattering $\beta(\lambda)$. The total attenuation loss coefficient, $c(\lambda)$ is (Jerlov, 1976):

$$c(\lambda) = \alpha(\lambda) + \beta(\lambda) \tag{1}$$

The absorption coefficient α (λ) is (Haltrin, 1999):

$$\begin{aligned} \alpha(\lambda) = a_w(\lambda) + a_c^0(\lambda).\left(\frac{C_0}{C_c^0}\right)^{0.602} \\ + a_f^0 C_f \exp(-k_f.\lambda) \\ + a_h^0 C_h \exp(-k_h.\lambda) \end{aligned} \tag{2}$$

where, $a_w(\lambda)$ is the pure water absorption coefficient whose value equal to 0.0257 m^{-1} for 500 nm; $a_c^0(\lambda)$ is the spectral absorption coefficient of chlorophyll with values equal to 0.0125 m^{-1} for 500 nm (Haltrin and Kattawar, 1991; Smith and Baker, 1981);

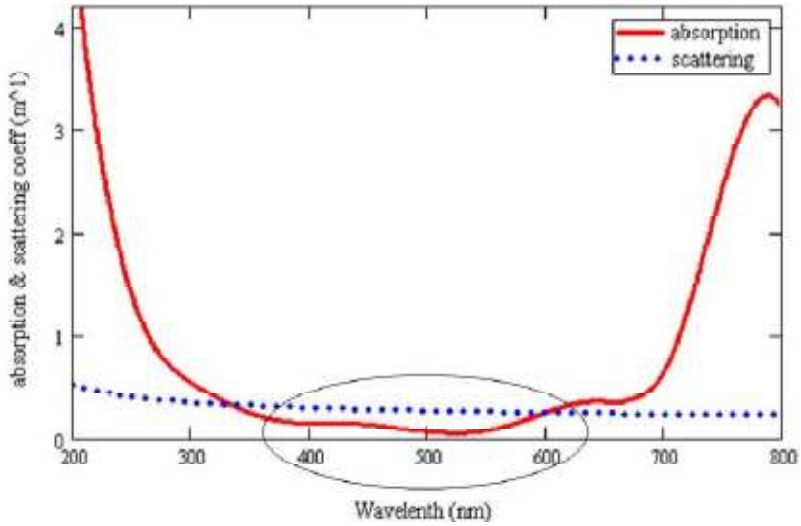

Fig. 1: Absorption and scattering coefficients of water with 1 mg/m^3 of chlorophyll concentration

Table 1: Chlorophyll concentration for different jerlov water types (Gawdi, 2006; Apel, 1987; Mobley *et al*., 2004)

Jerlov water type	Concentration of chlorophyll mg/m^3
I	0.03
II	1.25
III	3.00

$a_f^0 = 35.959 m^2/mg$ and $a_h^0 = 18.828 m^2/mg$ are the specific absorption coefficients of fulfic acid and humic acid, respectively; C_f and C_h are the concentration of the fulfic acid and humic acid, respectively; while k_f and k_h are constants whose values are 0.0189 and 0.01105 nm^{-1}, respectively. The concentrations of C_f and C_h are expressed through the chlorophyll concentration C_c as follows (Haltrin, 1999):

$$C_f = 1.74098 C_c \exp\left[0.12327\left(\frac{C_c}{C_c^0}\right)\right] \quad (3)$$

$$C_h = 0.19334 C_c \exp\left[0.12343\left(\frac{C_c}{C_c^0}\right)\right] \quad (4)$$

where, the constant with value equal to $C_c^0 = 1$ mg/m^3 and C_c is the total concentration of chlorophyll, which has different values depending on categories of Jerlov water types are shown in Table 1.

The mechanism of scattering process arises from pure water $\beta_w(\lambda)$, small particle $\beta_S^0(\lambda)$ and large particle $\beta_l^0(\lambda)$. Smalls particles have refractive index equal to 1.15, while large particles have a refractive index of 1.03 (Arnon and Kedar, 2009). The scattering coefficient is expressed as (Haltrin, 1999):

$$\beta(\lambda) = \beta_w(\lambda) + \beta_s^0(\lambda).C_s + \beta_l^0(\lambda).C_l \quad (5)$$

where, C_s and C_l are the concentrations of small and large particles, respectively and $\beta_w(\lambda)$, $\beta_S^0(\lambda)$ and $\beta_l^0(\lambda)$ are the scattering coefficients by the pure water, small particles and large particles, given by Haltrin (1999):

$$\beta_w(\lambda) = 0.005826\left(\frac{0.4}{\lambda}\right)^{4.322}, m^{-1} \quad (6)$$

$$\beta_s^0(\lambda) = 1.151302\left(\frac{0.4}{\lambda}\right)^{1.7}, m^2/g \quad (7)$$

$$\beta_l^0(\lambda) = 0.3411\left(\frac{0.4}{\lambda}\right)^{0.3}, m^2/g \quad (8)$$

where, C_s and C_l are the total concentration of small and large particles in g/m^3, respectively and can be expressed by:

$$C_s = 0.01739 C_c.\exp\left[0.11631\left(\frac{C_c}{C_c^0}\right)\right], g/m^3 \quad (9)$$

$$C_l = 0.76284 C_c.\exp\left[0.03092\left(\frac{C_c}{C_c^0}\right)\right], g/m^3 \quad (10)$$

Analysis of a link model:

Link budget: The received optical signal power P_r under Line of Sight (LOS) conditions is determined through empirical path loss models. The optical signal reaching the receiver is obtained by multiplying the

transmitter power, telescope gain and losses given by Arnon and Kedar (2009) as follows:

$$P_r = P_T \eta_T \eta_R \exp\left[-c(\lambda)\frac{d}{\cos(\theta)}\right] \times \frac{A_r \cos(\theta)}{2\pi d^2\left[1-\cos(\theta_0)\right]} \quad (11)$$

where,

P_t = The transmitted optical power
η_T and η_R = The optical efficiency of the T_x and R_x
$c(\lambda)$ = The attenuation coefficient
d = The perpendicular distance between the T_x plane and R_x plane
θ_0 = The T_x beam divergence angle
θ = The angle between the perpendicular to the R_x plane and the T_x-R_x trajectory
A_r = The receiver aperture area

Detection of optical radiation: When transmitted optical signals arrive at the receiver, they are converted to electronic signals by photo detectors. There are many types of photo detectors in existence, photodiodes are used almost exclusively in optical communication applications because of their small size, suitable material, high sensitivity and fast response time (Keiser, 2000). The types of photodiodes are the PIN photodiode and the Avalanche Photodiode (APD) because they have good quantum efficiency and are made of semiconductors that are widely available commercially. For optimal design of the receiver system, it is important to understand the characteristics of these photodiodes and the noise associated with optical signal detection (Trisno, 2006). The performance of an APD is characteristics by its responsivity $\Re_{APD}$. The average photocurrent generated by a steady photon stream of average optical power can be expressed (Keiser, 2004) as:

$$I_p = \Re_{APD} P_r = M \Re P_r \quad (12)$$

where, P_r is the average optical power received by the photo detector. The responsively $\Re$ for Si, Ge APD is equal to 75 and 35 A/W, respectively. The gain is designated by M and is equal to 150 and 50 for Si, Ge APD, respectively (Palais, 2004). The shot noise arises from the statistical nature of the production and collection of photoelectrons, for a photodiode the variance of the shot noise current I_{shot} in a bandwidth B_e is (Keiser, 2004):

$$\langle I_{shot}^2 \rangle = \sigma_{shot}^2 = 2qI_p M^2 F(M) \quad (13)$$

where, q is the electron charge and F (M) is the APD noise figure and equal to 0.5, 0.95 for Si, Ge APD (Ghassemlooy *et al*., 2013). The photodiode dark current arises from electrons and holes that are thermally generated at pn junction of the photodiode. If I_D is the dark current, then its variance is given by Keiser (2004):

$$\langle I_D^2 \rangle = \sigma_D^2 = 2qI_D M^2 F(M) B_e \quad (14)$$

For Si, Ge APD the dark current I_D is 15 and 700 nA, respectively (Palais, 2004) and bandwidth B_e is equal to 5 and 0.2 GHz for Si, Ge APD, respectively (Ghassemlooy *et al*., 2013). On the other hand, the thermal noise arises from the random motion of electrons that are always present at any finite temperature; consider a resistor that has a value R at temperature T. If $I_{thermal}$ is the thermal noise current associated with the resistor, then in a bandwidth B_e its variance $\sigma^2_{thermal}$ is (Keiser, 2004):

$$\langle I_{thermal}^2 \rangle = \sigma_{thermal}^2 = \frac{4k_B T}{R} B_e \quad (15)$$

The total noise current $\langle I^2_N \rangle$ can be written as (Keiser, 2004):

$$\langle I_N^2 \rangle = \langle I_{shot}^2 \rangle + \langle I_D^2 \rangle + \langle I_{thermal}^2 \rangle \quad (16)$$

The signal to noise ratio is given by Keiser (2004):

$$SNR = \frac{\langle I_P^2 M^2 \rangle}{\langle I_N^2 \rangle} = \frac{I_p^2 M^2}{2q(I_p + I_D)M^2 F(M) B_e + 4k_B T B_e / R} \quad (17)$$

BER for underwater communications: There are many types of modulation techniques which are suitable for optical communications. The formulas of BER can be expressed as a function of SNR:

- On-Off Keying (OOK) (Trisno, 2006):

$$BER_{NRZ-OOK} = \frac{1}{2} erfc\left(\frac{1}{2\sqrt{2}}\sqrt{SNR}\right) \quad (18)$$

$$BER_{RZ-OOK} = \frac{1}{2} erfc\left(\frac{1}{2}\sqrt{SNR}\right) \quad (19)$$

- Pulse Position Modulation (L-PPM) (Trisno, 2006; Popoola and Ghassemlooy, 2009):

$$BER_{L-PPM} = \frac{1}{2} erfc\left(\frac{1}{2\sqrt{2}} \sqrt{SNR \frac{L}{2} \log_2 L}\right) \quad (20)$$

- Pulse Amplitude Modulation (M-PAM) (Rouissat *et al*., 2012; Juanjuan *et al*., 2006):

$$BER_{M-PAM} = \frac{1}{2} erfc\left(\frac{\sqrt{SNR \log_2 M}}{2\sqrt{2}(M-1)}\right) \quad (21)$$

- Binary Phase Shift Keying (BPSK) (Hanzra and Singh, 2012):

$$BER_{BPSK} = \frac{1}{2} erfc\left(\sqrt{SNR}\right) \quad (22)$$

- Differential Phase Shift Keying (DPSK) (Robel and Mohmud, 2012):

$$BER_{DPSK} = \frac{1}{2} erfc\left(\frac{1}{\sqrt{2}} \sqrt{SNR}\right) \quad (23)$$

- Quadrature Phase Shift Keying (QPSK) (Hanzra and Singh, 2012):

$$BER_{QPSK} = erfc\left(\sqrt{SNR}\right) \quad (24)$$

- Quadrature Amplitude Modulation (H-QAM) (Rashed and Sharshar, 2014):

$$BER_{H-QAM} = \frac{2\left(1-\frac{1}{\sqrt{H}}\right)}{\log_2 H} erfc\left(\frac{3 \log_2 H (SNR)}{2(H-1)}\right) \quad (25)$$

where, L, M and H are the pulse position code, pulse amplitude code and quadrate amplitude code, respectively.

NUMERICAL RESULTS

In this section, using the above mentioned formulations the simulation is carried out to study the underwater optical channel and its effect on optical wireless communication employing different modulation techniques in the transmitter and APD receiver over underwater environment. The values of the simulation parameters and constants are given in Table 2.

Received signal power as a function of distance: In an underwater optical wireless communication system, communication distance is an important indicator. It is meaningful to study achievable distance d of optical beam under different water medium. Let us see the effect of the total attenuation coefficient c (λ) on the received optical power P_r based on Line of Sight model (LOS). Figure 2 shows curves of P_r as a function of distance d for three Jerlov water types specified in Table 1. In this case, the wavelength λ = 500 nm is used. Suppose there is the case of a tolerable loss of -150 dBm beyond which the signal is not detectable at the receiver. It noticed that, for Jerlov type III, the transmission range is limited to 5 m and 12 m for Jerlov type II waters. When the turbidity decreases Jerlov type I increases dramatically these ranges, obviously, it allows range to exceed 50 m.

Table 2: System parameters used in the simulation (Arnon and Kedar, 2009; Arnon, 2010; Vavoulas *et al*., 2014)

Parameter	Value
Transmission wavelength (λ)	500 nm
Transmitter power (P_T)	10 mw
Optical efficiency of transmitter η_T	0.75
Optical efficiency of receiver η_R	0.75
Laser beam divergence angle (θ_0)	60°
Transmitter inclination angle (θ)	5°
Receiver aperture area (A)	0.01 m^2
Electron charge (q)	1.6×10^{-19} C
APD load resistance (R)	10 kΩ
Boltzmann constant (k_B)	1.38×10^{-23} J.K
Temperature (T)	298 K

The factual increase of achievable transmission distance occurs when the chlorophyll concentration decreases. It is concluded that when a water quality is good, improvement increase occurs in achievable transmission distance significantly.

SNR for different water types: The SNR for Jerlov water type I is calculated in Fig. 3 using Si, Ge APD receiver. The SNR is increasing with the increasing power of the transmitter and decreasing with increasing distance link. It is believed that Ge APD presented the high SNR compared with the Si APD under the same operating conditions, the difference in characteristics of SNR curves between Si and Ge APD is about 1 dB.

BER characteristics of underwater optical wireless communications: BER plays a crucial role in an optical communication system. Here simulation results are presented to compare the performance of the optical modulation techniques under different Jerlov water types. On the other hand, we consider Si, Ge APD on the receiver side.

The impact of the distance of transmission:

Case of Si APD: Let us consider the BER performance as a function of the distance of transmission. Figure 4 shows the curves of the BER for different modulation techniques under jerlov water type I when a Si APD is used at the receiver. In this case, it is noticed that for BER 10^{-10}, the distance transmission is limited to 11 and 13 m for NRZ-OOK and RZ-OOK, respectively. For L-PPM the distance is about 14.5 m for L = 2 and it increases for larger L it becomes about 17 m for L = 4. It is noticed that for L = 4 we have the same performance as the DPSK. An improvement increase occurs when QAM was used as a modulation technique, where the distance of data transmission increases and reaches to 19 m and 20 m for 8-QAM and 4-QAM. In Fig. 5 and 6 it is assumed that the underwater optical

wireless communication operating in jerlov water conditions II, III, has chlorophyll concentration of 1.25 and 3 mg/m^3, respectively. It is clear that from

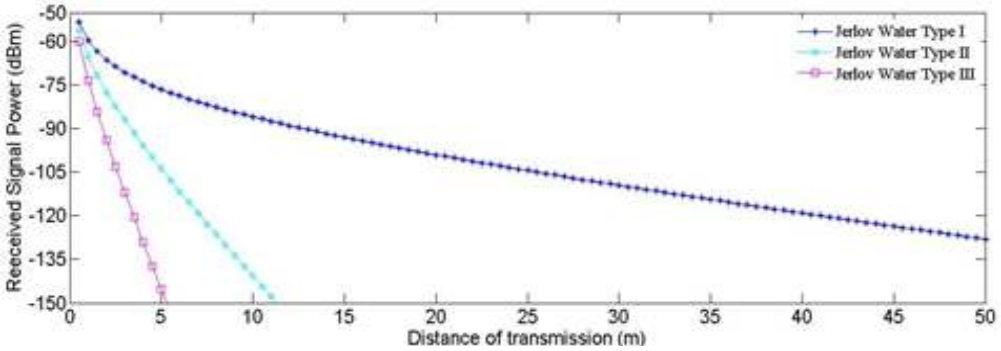

Fig. 2: Received signal power (dBm) for different jerlov water types

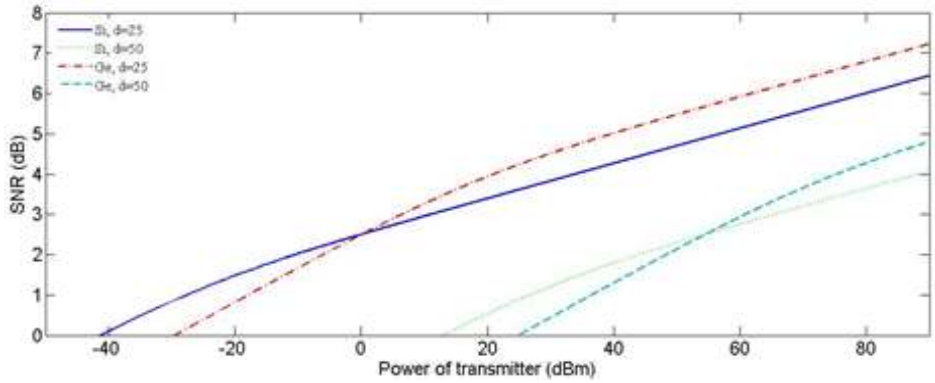

Fig. 3: SNR versus power of transmitter for jerlov water I

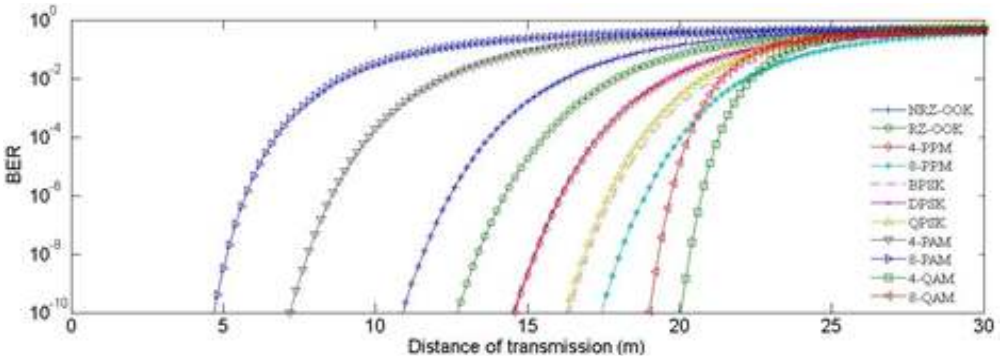

Fig. 4: BER performance for different modulations in jerlov water type I, Si APD

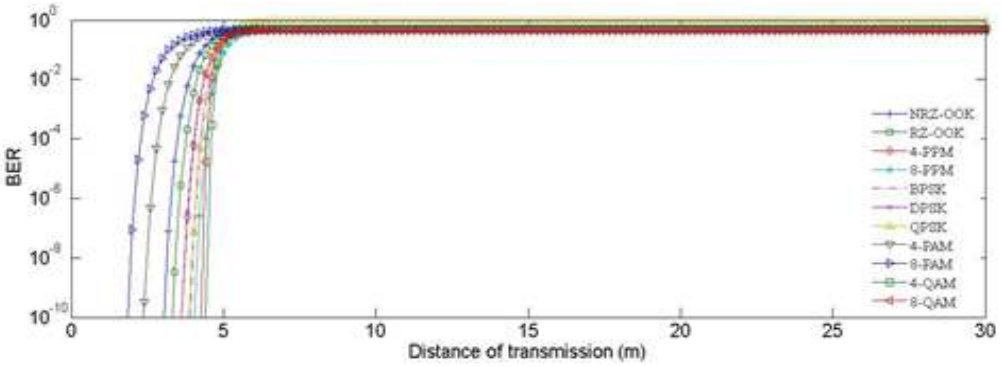

Fig. 5: BER performance for different modulations in jerlov water type II, Si APD

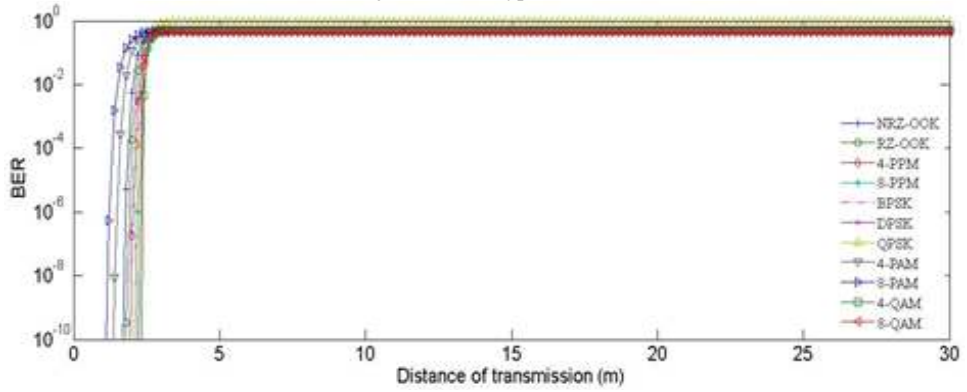

Fig. 6: BER performance for different modulations. Jerlov water type III, Si APD

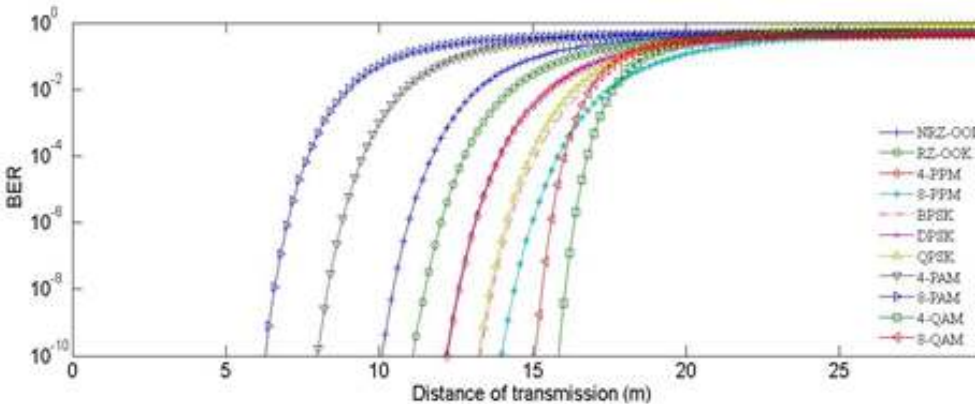

Fig. 7: BER performance for different modulations. Jerlov water type I, Ge APD

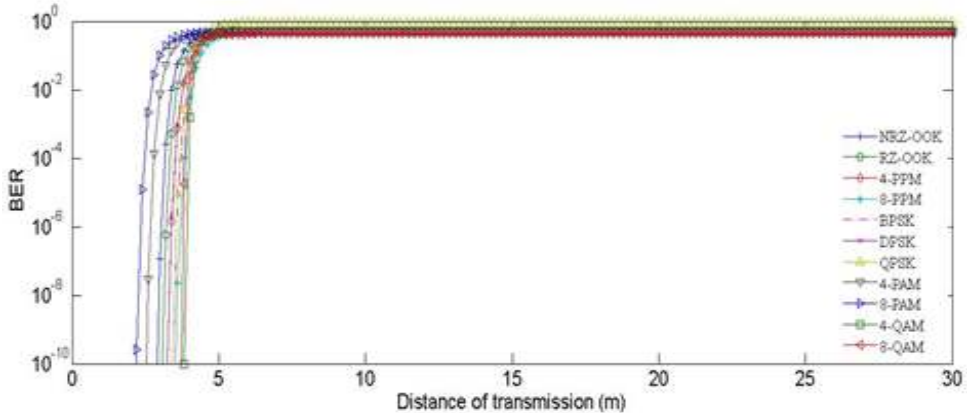

Fig. 8: BER performance for different modulations. Jerlov water type II, Ge APD

Fig. 5 and 6 there is no difference in BER curves for the modulation techniques under study. In this case, the data of the transmission do not exceed 4.5 and 3 m for jerlov water II, III, respectively. This decrease in distance of data transmission comes from increase in chlorophyll concentration.

Case of Ge APD: Another important simulation is to evaluate the performance of BER for Ge APD on the receiver side. It is noticed in Fig. 7 a significant decrease in the distance of transmission can be achieved by using different modulation techniques, the maximum data transmission is about 16 and 15 m for 4-QAM and 8-QAM, respectively. On the other hand, the distance in

the data transmission decrease for the other modulation techniques. The receiver sensitivity of M-PAM is lower than that of the other modulation techniques, therefore the BER performance of M-PAM is poor.

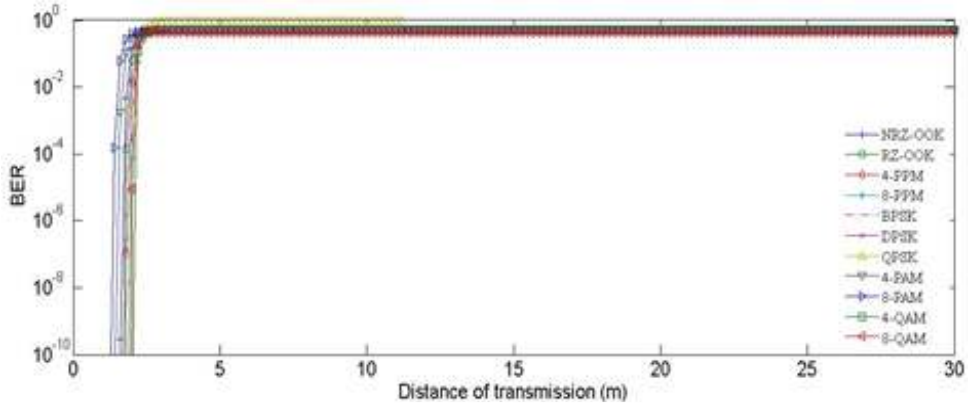

Fig. 9: BER performance for different modulations. Jerlov water type III, Ge APD

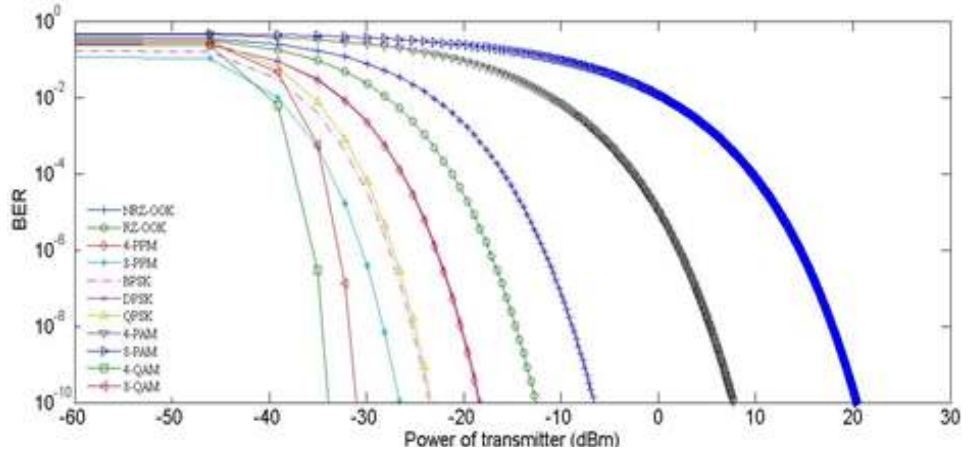

Fig. 10: BER versus power of transmission (dBm), Si APD, d = 25 m, jerlov type I

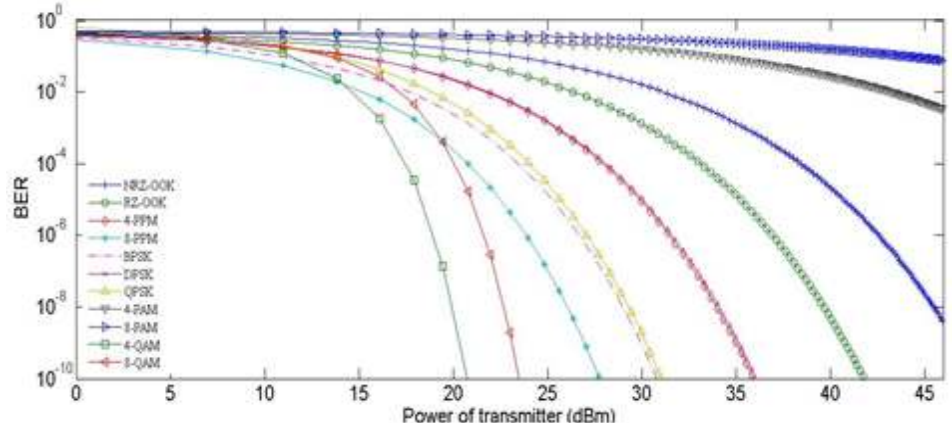

Fig. 11: BER versus power of transmission (dBm), Si APD, d = 50 m, jerlov type I

When a jerlov types II and III are applied as a communication medium as shown in Fig. 8 and 9, it is clear that there is no difference in BER curves for different modulation techniques. The maximum data transmission reached to 2 and 4 m for jerlov types II and III, respectively. It is worth noticing that for jerlov water types II and III as a communication medium, an approximation occurs in the BER performance for Si and Ge APD.

The impact of the power of transmitter:

Case of Si APD: The effect of power transmitter on BER is investigated. The performance of modulation techniques is compared when a Jerlov water type I is used with different link distances. Figure 10 shows the BER versus the power of the transmitter when the distance of transmission is d = 25 m. If we consider a required BER 10^{-10}, the power of transmitter is about 20 dBm, for 8-PAM and -35 dBm for 4-QAM. When the distance increases, as is evident in Fig. 11, the underwater optical communication system depends on the distance of transmission. An increase in the distance of transmission (d = 50 m) leads to an increase in the required power of transmission reaching more than 45 and 21 dBm for 8-PAM and 4-QAM, respectively for a target BER of 10^{-10}.

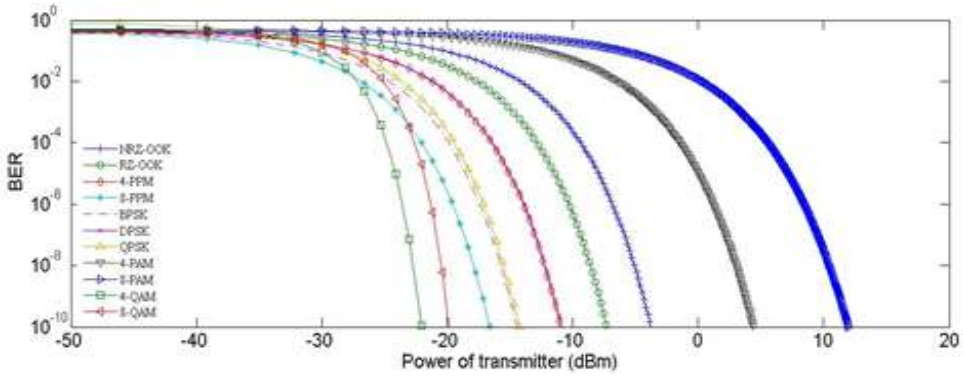

Fig. 12: BER versus power of transmission (dBm), Ge APD, d = 25 m, jerlov type I

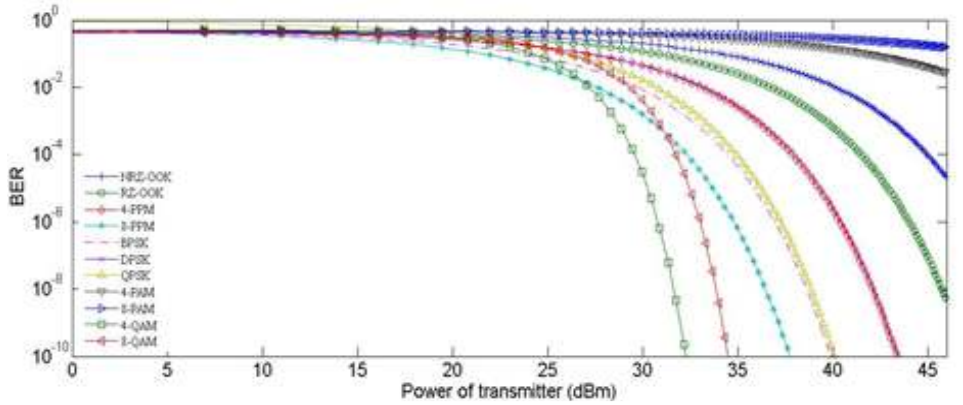

Fig. 13: BER versus power of transmission (dBm), Ge APD, d = 50 m, jerlov type I

Case of Ge APD: The same calculations were performed for Ge APD under Jerlov type I as a communication medium. Figure 12 shows BER for distance d = 25 m. For a target BER of 10^{-10}, the power of transmitter is about 12 and -22 dBm for 8-PAM, 4-QAM, respectively. This behavior of the curves leads to increase in the required power of the transmitter when Ge APD are applied. An analogous situation is Fig. 13, when a distance of transmission d = 50 m. If the required BER of 10^{-10} is considered, the power of transmitter reached to 33 dBm which is more than 45 dBm for 4-QAM, 8-PAM. It is concluded that when the distance increases the required power of transmitter is increases.

CONCLUSION

This study provides a theoretical performance analysis of an underwater optical wireless communication link using different modulation techniques in the transmitter and APD as a receiver with precisely aligned LOS geometry model for Jerlov water types. The attenuation coefficient of the laser beam through an underwater environment have a significant effect on the performance of underwater communication systems. The attenuation coefficients of water are compared with different Jerlov water types. Also, the effect of chlorophyll concentration and the distance of communication are investigated. The suitable choice of wavelength has a strong influence on the received optical power and SNR, which leads to long transmission in water. When a water have been increasing in chlorophyll concentration, this causes a decrease in received optical power and SNR, where a Si and Ge APD are employed on the receiver side. The SNR decreases with increase of distance and a minor

difference is observed between Si and Ge curves for jerlov water type under study. The BER characteristics of the different modulation techniques are studied. The results show that the QAM technique has a greater advantages than the others for Jerlov type I. On the other hand, a Si APD is more suitable receiver than Ge APD. When a Jerlov types II and III applied as a communication medium, the BER for a Si APD has the analogous behavior to that of Ge APD. The performance of BER is compared with the power of the transmitter (dBm) when a Si and Ge APD are used as a detector with different link distances. Therefore, the advantages of Si APD over Ge APD is approximately -13 and 12 dBm for distances 25 and 50 m, respectively, when we applied modulation technique 4-QAM is applied at BER 10^{-10}.

REFERENCES

Apel, J.R., 1987. Principles of Ocean Physics. Academic Press Inc., London, pp: 580-585.

Arnon, S., 2010. Underwater optical wireless communication network. Opt. Eng., 49(1).

Arnon, S. and D. Kedar, 2009. Non-line-of-sight underwater optical wireless communication network. J. Opt. Soc. Am. A, 28(3).

Gabriel, C., M.A. Khalighi, S. Bourennane, P. Léon and V. Rigaud, 2011. Channel modeling for underwater optical communication. Proceeding of IEEE GLOBECOM Workshops on Optical Wireless Communications. Houston, TX, pp: 833-837.

Gawdi, Y.J., 2006. Underwater free space optics. M.S. Thesis, North Carolina State University, Raleigh, NC.

Ghassemlooy, Z., W. Popoola and S. Rajbhandari, 2013. Optical Wireless Communications. System and Channel Modelling with MATLAB. CRC Press, Taylor and Frances Group, Boca Raton, FL.

Haltrin, V.I., 1999. Chlorophyll-based model of sea water optical properties. Appl. Optics, 38: 6826-6832.

Haltrin, V.I. and G.W. Kattawar, 1991. Effects of Raman scattering and fluorescence apparent optical properties of seawater. Report, Department of physics, Texas A&M University, College Station, TX.

Hanzra, T.S. and G. Singh, 2012. Performance of free space optical communication system with BPSK and QPSK modulation. IOSR J. Electron. Commun. Eng., 1(3): 38-43.

Jerlov, N.G., 1976. Marine Optics. Elsevier Scientific Publications, Amsterdam, New York, pp: 13-63.

Juanjuan, Y., Z. Zheng, H. Weiwei and X. Anshi, 2006. Improved performance of M-ary PPM free-space optical communication systems in atmospheric turbulence due to forward error correction. Proceeding of the 10th International Conference on Communication Technology (ICCT, 2006). Guilin, pp: 1-4.

Keiser, G., 2000. Optical Fiber Communications. McGraw-Hill Co., NY.

Keiser, G., 2004. Optical Essential Communications. McGraw-Hill Co., NY.

Mobley, C.D., 1994. Light and Water: Radiative Transfer in Natural Waters. Academic Press, San Diego, CA, pp: 592.

Mobley, C.D., D. Stramski, P.W. Bissett and E. Boss, 2004. Optical modeling of ocean waters: Is the Case 1 - Case 2 classification still useful? Oceanography, 17(2): 60-67.

Mullen, L., A. Laux and B. Cochenour, 2009. Propagation of modulated light in water: Implications for imaging and communications systems. Appl. Optics, 48(4).

Palais, K.C., 2004. Fiber Optic Communications. 4th Edn., Prentice-Hall Inc., NY.

Pignieri, F., F. De Rango, F. Veltri and S. Marano, 2008. Markovian approach to model underwater acoustic channel: Techniques comparison. Proceeding of the Military Communications Conference (MILCOM). San Diego, CA, pp: 1-7.

Popoola, W.O. and Z. Ghassemlooy, 2009. BPSK subcarrier intensity modulated free-space optical communications in atmospheric turbulence. J. Lightwave Technol., 27(8): 967-973.

Rashed, A.N.Z. and H.A. Sharshar, 2014. Deep analytical study of optical wireless communication systems performance efficiency using different modulation techniques in turbulence communication channels. Int. J. Adv. Res. Electr. Comm. Eng., 3(3).

Robel, M.M.H. and S.G. Mohmud, 2012. BER performance analysis for optical communication using DPSK modulation. Int. J. Comput. Appl., 59(9).

Rouissat, M., R.A. Borsali and M.C. Bled, 2012. Dual amplitude width PPM for free space optical systems. Int. J. Inform. Technol. Comput. Sc., 3: 45-50.

Shah, G., 2009. A survey on medium access control in underwater acoustic sensor networks. Proceeding of the International Conference Workshops on Advanced Information Networking and Applications (WAINA). Bradford, UK, pp: 1178-1183.

Smith, R.C. and K.S. Baker, 1981. Optical properties of the clearest natural waters. Appl. Optics, 20: 177-184.

Tang, S., X. Zhang and Y. Dong, 2013. On impulse response for underwater wireless optical links. Proceeding of the IEEE Oceans Conferences-Bergen, MTS/IEEE.

Trisno, S., 2006. Design and analysis of advanced free space optical communication systems. Ph.D. Thesis, University of Maryland.

Vavoulas, A., H.G. Sanalidis and D. Varoutas, 2014. Underwater optical wireless networks: A k-

connectivity analysis. IEEE J. Oceanic Eng., 39(4): 801-809.